The Major Cyclic Trimeric Product of Indole-3-carbinol Is a Strong Agonist of the Estrogen Receptor Signaling Pathway†

Jacques E. Riby,‡ Chunling Feng,‡ Yu-Chen Chang,‡ Charlene M. Schaldach,‡ Gary L. Firestone,§ and Leonard F. Bjeldanes*,‡

Division of Nutritional Sciences and Toxicology, and Department of Molecular and Cell Biology, University of California, Berkeley, California 94720

Received August 23, 1999; Revised Manuscript Received November 15, 1999

ABSTRACT: Indole-3-carbinol (I3C), a component of *Brassica* vegetables, is under study as a preventive agent of cancers of the breast and other organs. Following ingestion, I3C is converted to a series of oligomeric products that presumably are responsible for the in vivo effects of I3C. We report the effects of the major trimeric product, 5,6,11,12,17,18-hexahydrocyclonona[1,2-*b*:4,5-*b*′:7,8-*b*″]triindole (CTr), on the estrogen receptor (ER) signaling pathways. Tumor-promoting effects of high doses of I3C may be due to activation of aryl hydrocarbon receptor (AhR)-mediated pathways; therefore, we also examined the effects of CTr on AhR activated processes. We observed that CTr is a strong agonist of ER function. CTr stimulated the proliferation of estrogen-responsive MCF-7 cells to a level similar to that produced by estradiol (E_2) but did not affect the growth of the estrogen-independent cell line, MDA-MD-231. CTr displaced E_2 in competitive-binding studies and activated ER-binding to an estrogen responsive DNA element in gel mobility shift assays with EC_{50}s of about 0.1 μM. CTr activated transcription of an E_2-responsive endogenous gene and exogenous reporter genes in transfected MCF-7 cells, also with high potency. CTr failed to activate AhR-mediated pathways, consistent with the low-binding affinity of CTr for the AhR reported previously. Comparisons of the conformational characteristics of CTr with other ER ligands indicated a remarkable similarity with tamoxifen, a selective ER antagonist used as a breast cancer therapeutic agent and suggest an excellent fit of CTr into the ligand-binding site of the ER.

Indole-3-carbinol (I3C),[1] a hydrolytic product of glucobrassicin found in common *Brassica* vegetables, is under study as a tumor preventive agent (*1*−*3*). Some of the most pronounced effects of I3C have been reported to be against tumor development in estrogen-responsive tissues. When administered prior to and during treatment with direct- and indirect-acting mammary carcinogens, I3C reduced tumor incidence by as much as 95% (*4*, *5*). I3C is also reported to inhibit spontaneous formation of tumors of the mammary gland and of the endometrium of rodents (*6*, *7*). At high doses, I3C promotes tumorigenesis in the thyroid gland, colon, pancreas, and liver of rodents when administered following treatment with a carcinogen (*8*−*10*). A recent report indicates that I3C exhibits tumor-promoting activity in the trout model in a range of concentrations below that which is required to induce the cytochrome P450 pathways thought to be important in the cancer protective effects of I3C (*11*). Clearly, if I3C is to be developed further as a cancer protective agent, its modes of action as a tumor-preventive and tumor-promoting agent must be thoroughly understood.

In our continuing efforts to examine the mechanisms of action of I3C, we have begun to determine the biological activities of the components of the acid reaction mixture (RXM) of I3C. It is now well-established that I3C is highly unstable in gastric acids and is rapidly converted to a mixture of oligomeric products following ingestion (*12*, *13*). I3C products found in vivo include indolo[3,2-*b*]carbazole (ICZ), a minor product that is a potent activator of Ah receptor pathways and exhibits antiestrogenic activities, DIM, a major product that is a potent inhibitor of carcinogen-induced mammary tumorigenesis in rodents and a weak activator of the Ah receptor, and LTr, a second major product and an antagonist of estrogen receptor function that inhibits proliferation of both estrogen-dependent and -independent cultured breast tumor cells (*14*−*19*). We report here the effects of the third major component of RXM, the cyclic trimeric product, 5,6,11,12,17,18-hexahydrocyclonona[1,2-*b*:4,5-*b*′:7,8-*b*″]triindole (CTr), on pathways mediated by the estrogen receptor and the Ah receptor in tumor cells. We show that this indole product is a strong agonist of estradiol (E_2) functions including estrogen receptor binding and activation and induction of proliferation of estrogen-dependent cultured breast tumor cells and transcriptional activation of E_2-

† This work was supported by the Department of Defense, Army Breast Cancer Research Program Grant DAMD17-96-1-6149 and by Grant CA69056 from the National Institutes of Health.

* Corresponding author: Leonard F. Bjeldanes, Division of Nutritional Sciences and Toxicology, 119 Morgan Hall, University of California at Berkeley, Berkeley, CA 94720. Telephone: 510-642-1601. Fax: 510-642-0535. E-mail: lfb@nature.berkeley.edu.

‡ Division of Nutritional Sciences and Toxicology.

§ Department of Molecular and Cell Biology.

[1] Abbreviations: I3C, indole-3-carbinol; CTr, 5, 6, 11, 12, 17, 18-hexahydrocyclonona[1, 2-*b*: 4, 5-*b*′: 7, 8-*b*″]triindole; E_2, 17-β-estradiol; ER, estrogen receptor; ERE, estrogen receptor responsive element; AhR, aryl hydrocarbon receptor; DIM, 3,3′-diindolylmethane; ICZ, indolo-[3, 2-*b*]carbazole; LTr-1, 2-(indol-3-ylmethyl)-3, 3′- diindolylmethane; EROD, ethoxyresorufin O-deethylase; OHT, 4-hydroxytamoxifen.

10.1021/bi9919706 CCC: $19.00
Published on Web 01/14/2000

responsive genes. In contrast, CTr exhibited weak activities in measures of Ah receptor activation that were consistent with the low-binding affinity we have reported previously for this receptor (*13*). Conformational comparisons indicated that CTr is similar to the established therapeutic agent, tamoxifen, and that CTr fits strickingly well into the ligand-binding site of the ER.

EXPERIMENTAL PROCEDURES.

Preparation of Acid Reaction Mixture (RXM). The procedure reported by Gross and Bjeldanes (*12*) was followed for the preparation of RXM. Briefly, I3C (100 mg, Aldrich Chemical Co., Milwaukee, WI) was suspended in 1 M HCl (100 mL) at room temperature for 15 min. The acid suspension was neutralized with aqueous ammonia to pH 7.0, and the precipitate was filtered and dried under vacuum to give RXM as a reddish powder.

Isolation CTr from RXM. RXM (200 mg) was dissolved in 1 mL of THF and fractionated initially by silica gel vacuum liquid chromatography. Mixtures of hexane/THF with increasing polarity were used as mobile phase to obtain the following five crude fractions: 100% hexane (A), hexane/THF 2:1 (B), hexane/THF 1:1 (C), hexane/THF 1:2 (D) and 100% THF (E). Fractions B and C, shown by analytical HPLC to contain CTr, were combined, extracted with hexane to remove highly lipophilic components, and resuspended in THF before injection onto semipreparative HPLC. HPLC purification of CTr was performed using a Shimadzu HPLC system (SCL-10A, Shimadzu Scientific Instruments, Inc., Japan) equipped with a C-18 bonded-phase semipreparative column (Beckman Ultrasphere-ODS, 10 × 250 mm, 5 mm) (Beckman, San Ramon, CA) and UV-vis detector (SPD-10AV, Shimadzu Scientific Instruments, Inc., Japan). Isocratic elution employed a mixture of acetonitrile/water (60:40) at a flow rate of 1.5 mL/min with the detector setting at 280 nm. The electron impact mass spectrometry analyses of the HPLC fractions of interest were performed at the Mass Spectrometry Facility of the College of Chemistry, University of California at Berkeley. The isolated CTr gave a single peak on analytical HPLC with the expected mass spectrum (*12*).

Cell Culture. The human breast adenocarcinoma cell lines, MCF-7 and MDA-MB-231, and the murine hepatoma cell line, Hepa-1c1c7, obtained from the American Type Culture Collection (ATCC, Maryland, U.S.A.), were grown as adherent monolayers in Dulbecco's modified Eagle's medium (DMEM), supplemented with 10% fetal bovine serum and passaged at approximately 80% confluence. Cultures of human cells were used in subsequent experiments for fewer than 25 passages.

Cell Proliferation. Before the beginning of the treatments, cells were depleted of estrogen for 7−10 days in medium composed of phenol-red-free DMEM supplemented with 5% calf serum twice stripped in dextran-coated charcoal, 0.1 nM nonessential amino acids, 2 mM glutamine and 10 ng/mL insulin. During the depletion period, medium was changed every other day. Treatments were administered by addition of 1 μL of 1000X solutions in DMSO per mL of medium. Once the treatment period started, medium was changed daily to counter possible loss of readily metabolized compounds. Cells were harvested by trypsinization and counted in a Coulter (Miami, FL) particle counter.

Estrogen Receptor (ER) Binding Assay. Rat uterine cytosol was prepared as described previously (*20*). Briefly, 2.5 g of uterine tissue from five Sprague−Dawley rats (12 weeks old) was excised and placed on ice. The fresh tissue was homogenized with 30 mL of ice-cold TEDG buffer (10 mM Tris, pH 7.4, 1.5 mM EDTA, 1 mM DTT, 10% glycerol) using a Polytron at medium speed for 1 min on ice. The homogenate was centrifuged at 1000*g* for 10 min at 4 °C. The supernatant solution was transferred to ultracentrifuge tubes and centrifuged at 100 000*g* for 90 min at 4 °C. The supernatant solution was divided into 1.0 mL aliquots, quickly frozen in a dry ice/ethanol bath, and stored at −80 °C. Protein concentration of the uterine cytosol was measured by the Bradford assay using bovine serum albumin as the standard. For each competitive-binding assay, 5 μL of 20 nM ^{3}H-E_2 in 50% ethanol, 10 mM Tris, pH 7.5, 10% glycerol, 1 mg/mL BSA, and 1 mM DTT was placed in a 1.5 mL microcentrifuge tube. Competitive ligands E_2 (0.1 nM−1.9 μM), ICI_{182780} (0.1 nM−5.0 μM), and CTr (1.0 nM−10 μM) were added as 1.0 μL of 100X solution in DMSO. After the solution was mixed, 95 μL of uterine cytosol was added, the solutions were vortexed and incubated at room temperature for 2−3 h. Proteins were precipitated by addition of 100 μL of 50% hydroxylapatite slurry equilibrated in TE (50 mM Tris, pH 7.4, 1 mM EDTA) and incubation on ice for 15 min with vortexing every 5 min to resuspend hydroxylapatite. The pellet was washed with 1.0 mL ice-cold wash buffer (40 mM Tris, pH 7.4, 100 mM KCl), and centrifuged for 5 min at 10 000 rpm at 4 °C. The supernatant was carefully aspirated and the pellet washed two more times with 1.0 mL of wash buffer. The final pellet was resuspended in 200 μL ethanol and transferred to a scintillation vial. The tube was washed with another 200 μL portion of ethanol, which was then added to the same counting vial. A negative control contained no uterine cytosol. Nonspecific binding was determined using 1000-fold excess of unlabeled E_2. Data points were connected by a Bezier curve and EC_{50} values were determined graphically as the concentration of competitor needed to reduce ^{3}H-E_2 binding by 50%.

Reporter Plasmids and Expression Vectors. The ER-responsive CAT reporter plasmids pERE-vit-CAT and pATC2 (*21*) were gifts from D. J. Shapiro (University of Illinois, Urbana-Champain). pERE-vit-CAT contains the 5′-flanking and promoter region (−596 to 21) of the *Xenopus* vitellogenin-B1 gene, including two imperfect endogenous EREs (at −302 and −334) and an exogenous consensus ERE (GGTCACAGTGACC) inserted at position −359. The simpler reporter pATC2 contains two copies of the consensus ERE coupled 38 bp from the TATA box of the vitellogenin-B1 promoter (−42 to 14). The luciferase reporter plasmid pS2-luc (*22*) containing the 5′-flanking region (−537 to −87) of the human pS2 gene upstream of the SV40 promoter and the firefly luciferase stuctural gene was a gift from T. Zacharewski (University of Western Ontario, London Ontario, Canada). The plasmid pCMV-hER constitutively expressing a fully functional human estrogen receptor (*23*) was a gift from B. S. Katzenellenbogen (University of Illinois, Urbana-Champain). The transfection efficiency control vector, pCMVβ constitutively expressing β-galactosidase, was obtained from ATCC.

Transient Transfections with Reporters. Transfections were done using Lipofectamine (Gibco BRL). Cells were grown in 10% FBS-DMEM until 80% confluent and transferred to 6.0 cm Petri plates 24 h before transfection. The plates were seeded with the appropriate number of cells to be 50−60% confluent at the time of transfection. For each 6 cm plate, 8 μL of lipofectamine was diluted with 92 μL of serum free medium. Plasmid DNA (0.1 μg luciferase reporter DNA per plate and 1.0 μg CAT reporter DNA per plate) was diluted in 100 μL of a serum-free medium. Lipid and plasmid dilutions were combined, mixed gently, and incubated at room temperature for 30−45 min. Meanwhile, the plates were washed with 4 mL serum free medium and 2 mL serum free medium was added to each plate. The 200 μL of the lipid/DNA suspension was added to each plate and mixed gently. The plates were returned to the incubator for 5−6 h and 2 mL of medium containing 10% calf serum was added. The next day, the plates were treated with fresh stripped medium without phenol-red (5% DCC−FBS) and the 48 h treatments were started by addition of 1 μL of 1000X solutions in DMSO per mL of medium. The transfection efficiency was determined using the constitutive galactosidase expression plasmid pCMVβ in an identical set of plates and was found to be unaffected by the treatments.

Chloramphenicol Acetyl Transferase (CAT) Assay. The CAT assay was done using a modification of the phase extraction assay described by Seed et al. (*24*). At the end of the 48 h treatment period, the transfected cells were harvested by scrapping with a rubber policeman, transferred with the medium to a conical 15 mL tube, centrifuged at 600*g* for 2 min, resuspended in 1 mL cold PBS, transferred to Eppendorf tubes, centrifuged at 600*g* for 2 min and washed in PBS a second time. Cell pellets were resuspended in 200 μL of Tris (0.1 M, pH 8.0) and lysed by 3 cycles of freeze−thaw treatment (alternating 5 min in a dry ice/alcohol bath and 5 min in a 37 °C bath). Cell lysates were incubated at 65 °C for 15 min to inactivate acylases and centrifuged at 14 000*g* for 8 min. A 165 μL aliquot of the cytosol was transferred to a 7 mL scintillation vial, and a 20 μL aliquot was reserved for determination of protein concentration by the Bradford assay. The substrate mixture (85 μL) was added to the scintillation vial for final concentrations of 100 mM Tris-HCl, pH 8.0, 250 nmoles chloramphenicol, 1 μCi ^{3}H-acetylCoA (200 mCi/mmol) in a total volume of 250 μL and mixed thoroughly. The organic scintillation fluid (4 mL) was added slowly and the vials were incubated at 37 °C for 1−2 h or until sufficient counts were obtained.

RNA Extraction and Northern Blot Analysis of pS2 Expression. Cells were lysed by addition of Tri-reagent (Molecular Research Center, Inc., Cincinnati, OH), and chloroform was used for phase separation. After centrifugation, the water-soluble upper phase was collected and total RNA was precipitated with 2-propanol, washed with 75% ethanol, and dissolved in DEPC-treated water. Total RNA was electrophoresed on a 1.2% agarose gel containing 3% formaldehyde, using MOPS as the running buffer. The gel was then washed gently with 10X SSC and blotted with a Zeta nylon membrane (Biorad, Hercules, CA) overnight. The RNA was fixed to the membrane by UV cross-linking. The hybridization probes were radio-labeled with (α^{32}P) dCTP using random primers and the pS2-cDNA and GAPDH-cDNA plasmids provided by ATCC as the template. Hybridization and quantitation of results were done as described previously (*15*). Specific pS2 mRNA levels were normalized using GAPDH as a standard.

Nuclear Extracts. Three near confluent (80−90%) cultures of MCF-7 cells in 100 mm Petri dishes were used for each treatment. CTr or E_2 was added as 1 μL of 1000X solution in DMSO per mL of medium. After 2 h of incubation at 37 °C, the plates were placed on ice and washed twice with 5 mL of hypotonic buffer (10 mM Hepes, pH 7.5) and incubated with 2 mL of the same buffer for 15 min. Cells were harvested in 1 mL of MDH buffer (3 mM $MgCl_2$, 1 mM DTT, 25 mM Hepes, pH 7.5) with a rubber scrapper, homogenized with a loose fitting Teflon pestle, and centrifuged at 1000*g* for 4 min at 4 °C. The pellets were washed twice with 3 mL of MDHK buffer (3 mM $MgCl_2$, 1 mM DTT, 0.1 M KCl, 25 mM Hepes, pH 7.5), resuspended in 1 mL of MDHK, and centrifuged at 600*g* for 4 min at 4 °C in a microcentrifuge. The pellets were resuspended in 100 μL of HDK buffer (25 mM Hepes, pH 7.5, 1 mM DTT, 0.4 M KCl), incubated for 20 min on ice with mixing every 5 min, and centrifuged at 14000*g* for 4 min at 4 °C. Glycerol was added to the supernatants to a concentration of 10% and aliquots of the nuclear extracts were stored at −80 °C.

Gel Mobility Shift Assay. The following set of complementary 31-mer oligonucleotides, 5′-GATCC*CAGGTCACAGTGACCTG*AGCTAAAAT-3′ and 5′-GATCATTTTAGCT*CAGGTCACTGTGACCTG*G-3′ containing the palindromic ERE consensus motif (italicized), was annealed and 5′-end labeled with (γ^{32}P)-ATP using T4 nucleotide kinase. The resulting labeled double-stranded DNA probe was purified on a Sephadex G50 spin-column, precipitated in ethanol, dissolved in TE buffer, and diluted in 25 mM Hepes, 1 mM DTT, 10% glycerol, 1 mM EDTA to contain approximately 25 000 cpm of ^{32}P/μL. Nuclear extracts (7 μg of proteins) were mixed with 90 ng poly-dIdC, 25 mM Hepes, 1 mM DTT, 10% glycerol, 1 mM EDTA, 160 mM KCl in a total volume of 21 μL. For antibody supershift experiments, 0.5 μg of monoclonal mouse-IgG anti-human-ER (Santa Cruz Biotechnology, Santa Cruz, CA) was added to the incubation mixture. After incubation for 15−20 min at room temperature, 4 μL (100 000 cpm) of an end-labeled ^{32}P-ERE probe was added and incubated for another 15 min at room temperature. After addition of 2.8 μL of 10X ficoll loading buffer (0.25% bromophenol blue, 25% ficoll type 400), 22 μL aliquots were loaded unto a pre-run, nondenaturing 4.0% polyacrylamide gel in TAE (67 mM Tris, 33 mM sodium acetate, 10 mM EDTA, pH 8.0) at 120 V for 2 h. The gel was then dried and autoradiographed.

Ethoxyresorufin O-Deethylase Assay. Enzymatic activity of cytochrome-P4501A1 was measured by the ethoxyresorufin O-deethylase (EROD) assay as described previously (*15*). Briefly, after the 18−24 h treatment, cells were trypsinized and 5 mL of PBS was added to the cells. The reaction was run at room temperature and the cells and the reaction solutions were first incubated at 37 °C. An aliquot of the cell suspension was counted to obtain the cell number and 1.5 mL of the cell suspension was added into a fluorometer cuvette, followed by the addition of 0.5 mL of 2.5 mM ethoxyresorufin (Sigma). The reaction mixture was mixed by inversion of the cuvette and fluorescence was measured

at the excitation wavelength of 510 nm and emission wavelength of 586 nm with a 20 nm slit width using a Perkin-Elmer 650−10S spectrofluorometer. Chart speed was recorded for time determination, and a standard curve was obtained using resorufin (RF) (Sigma) added to the heat-inactivated control cells. The enzyme activity was then presented as pmole RF produced/minute/10^6 cells.

Modeling of CTr-binding to the ER Ligand Binding Domain. Since CTr is a strong agonist of estrogen receptor function but exhibits no obvious structural similarity to E_2, we compared the structure of CTr to other classes of ER ligands. Our comparisons included size or "steric" considerations and also electrostatic charge distribution observations. Quantum mechanical geometry optimizations were performed using GAMESS (*25*) on 17β-estradiol, raloxifene, tamoxifen, and CTr molecules; solvent-accessible surfaces were then constructed surrounding these molecules to enable the solution of the Poisson−Boltzmann equation as described previously (*26*). The electronic distribution of the molecule is allowed to rearrange in response to the polarization of its interface with an aqueous environment. The polarization charge induced on these surface elements is mapped onto the nodes ("dots") from which the surface is comprised. These calculations were performed at the 6-31G**/MP2 level of theory allowing for an accurate depiction of the induced surface charge density. The 6-31G** nomenclature is used to describe the basis set used in the calculations, which includes Pople's N-31G split valence basis set. MP2 refers to the Møller−Plesset second-order perturbation theory method of inclusion of electronic correlation (*27*).

We next placed each of these molecules into the experimentally determined ER-binding sites obtained by Brzozowski et al. and Shiau et al. from their complexing of the ER with the specific ligand and determining the respective crystal structure (*28*, *29*). The minimum energy configurations of the molecules were determined by varying both the positions of their centers of mass and their three-dimensional angular orientation within the binding sites. Atoms comprising the binding site itself were not allowed to relax. Interatomic potentials required for this minimization were determined by pairwise summation using local density methods and reflect the electronic overlap repulsion between the atoms comprising the molecule and those in the appropriate receptor-binding site (*30*).

RESULTS

Cell Growth Assays. The effects of CTr were examined on the proliferation of the estrogen-responsive breast cancer cell line, MCF-7, and the estrogen-independent cell line, MDA-MB-231. The results indicate (Figure 1) that after a five-day period in complete medium (DMEM-10% FBS), the growth of MCF-7 cells was significantly increased compared to the vehicle (DMSO)-treated controls at CTr concentrations from 10 nM to 1 μM. The proliferation of the MDA-MB-231 cells was not affected by CTr in this concentration range. In MCF-7 cells grown in an estrogen-depleted medium (5% DCC−FBS DMEM), CTr produced a maximum increase in cell number that was similar to that produced by E_2. Co-treatment of MCF-7 cells in a depleted medium with a range of concentrations of CTr and at the maximum effective concentration of E_2 did not alter the E_2-induced growth rates. These results suggest that CTr may possess estrogenic activity.

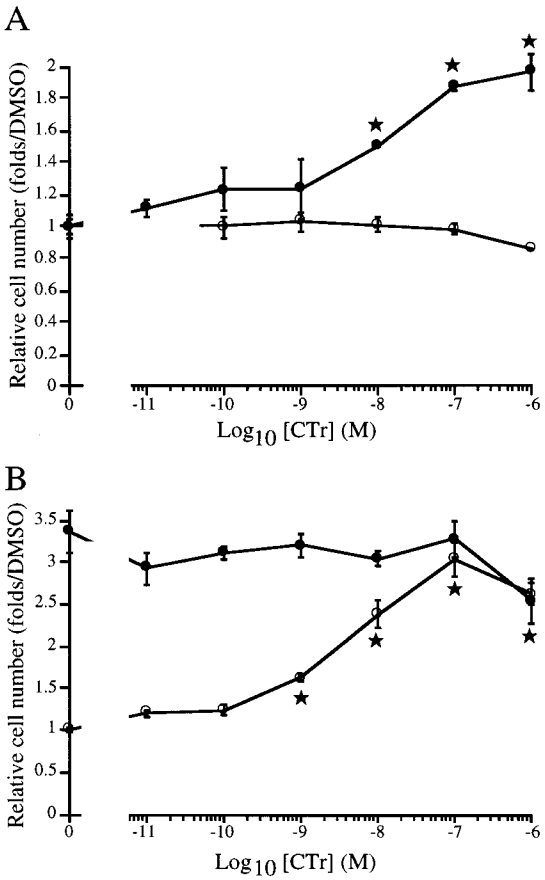

FIGURE 1: Effect of CTr on proliferation of breast cancer cells. Panel A: MCF-7 cells (closed circles) and MDA-MB-231 cells (open circles) were plated in 10% FBS-DMEM at a density of 10^5 cells per well in 6-well plates and treated with CTr at the concentrations indicated. Panel B: MCF-7 cells grown for 7 days in estrogen depleted medium were plated at a density of 10^5 cells per well in 6-well plates and treated with CTr at the concentrations indicated, in the presence (closed circles) or absence (open circles) of E_2 (1 nM). Duplicate aliquots of cells from individual wells were counted after 5 days. The results are shown as the average and standard deviation from three identical wells and expressed as the ratio of cell numbers over the corresponding DMSO controls. The statistical differences were determined using ANOVA and Tukey's Studentized Range test: (star) significantly different ($p < 0.05$) from DMSO control.

Competitive Estrogen Receptor (ER) Binding Assay. Because CTr exhibited estrogen-like activity in the cell proliferation assays, we examined the binding affinity of CTr with the ER using a competitive-binding assay. CTr displaced ^{3}H-labeled E_2 in a rat uterine cytosol binding assay producing a competitive-binding curve parallel to that of the other ER ligands and with an EC_{50} that was only 2 orders of magnitude greater than that of E_2 (Figure 2). The EC_{50} of the estrogen antagonist, ICI_{182780}, used as a positive control for this assay, correlates with its affinity for the ER. These results indicate that CTr is a strong ligand for the ER that binds to the E_2-binding site of the receptor.

Gel Mobility Shift Assay. To determine whether CTr can activate the binding of the ER to the corresponding estrogen-responsive element (ERE) in the regulatory region of E_2-responsive genes, we conducted a series of gel mobility shift assays. Nuclear protein extracts of MCF-7 cells grown in

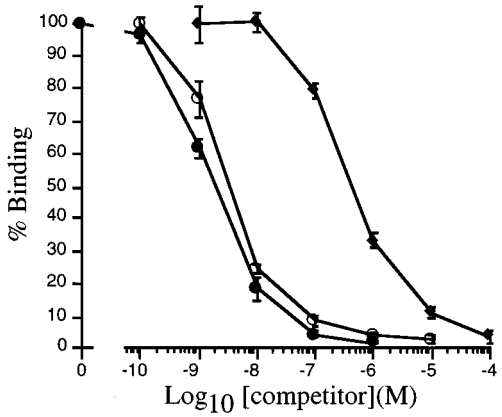

FIGURE 2: Competitive binding to the ER. The binding of $^3H-E_2$ (1 nM) to the ER from rat uterine cytosol was measured in the presence of the unlabeled competitors, E_2 (closed circles), ICI_{182780} (open circles), and CTr (closed diamond), at the concentrations indicated and reported as the percentage of binding in the absence of competitors. The results are shown as the average and standard deviation from three replicates. Relative binding affinities were calculated using the concentration of competitor needed to reduce ^3H-E_2 binding by 50% as compared to the concentration of unlabeled E_2 needed to achieve the same result.

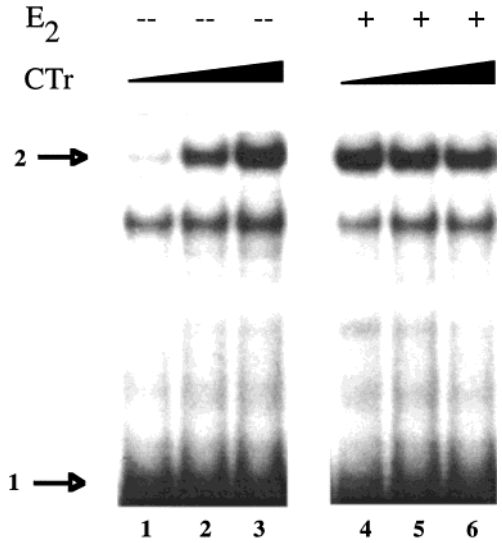

FIGURE 3: Binding of nuclear proteins to the ERE. Gel mobility shift analysis of nuclear extracts from estrogen depleted MCF-7 cells treated for 2 h with DMSO (lanes 1 and 4), CTr 10 nM (lanes 2 and 5), or CTr 100 nM (in lanes 3 and 6), and E_2 1 nM (lanes 4−6). A monoclonal antibody specific for the human ER was also added to the incubation mixture. Arrows indicate the locations of the free labeled probe (arrow # 1) and the ligand responsive antibody-super-shifted band (arrow # 2).

an estrogen-depleted medium for 7 days and treated for 2 h with CTr (10 nM and 100 nM) produced a shifted band with the ^{32}P-labeled consensus ERE oligonucleotide that was the same size as the ER−ERE complex induced by a 1 nM E_2 treatment. Figure 3 shows the complex supershifted by a monoclonal anti-ER antibody. The density of the shifted bands correlated with the concentrations of CTr and 100 nM CTr was as effective as 1 nM E_2. These results indicate that CTr can activate the ER into a DNA-binding form in a concentration range that corresponds to the binding affinity of CTr for the ER.

Activation of Transcription by CTr. To determine whether the binding of CTr with the ER produces a transcriptionally active complex with DNA, we examined by Northern blot assay whether CTr could activate expression of the endogenous E_2-responsive gene, pS2. Treatment of MCF-7 cells depleted of estrogen with CTr for 48 h at concentrations ranging from 10 nM to 1 μM induced accumulation pS2 mRNA in a concentration-dependent manner with 100 nM CTr as effective as 1 nM E_2 (Figure 4A). Co-treatment with CTr did not affect E_2-induced pS2 expression levels.

To examine whether the CTr-induced increase in pS2 mRNA levels could be attributed to an increase in transcriptional activity, we examined the effect of CTr on activities of three E_2-responsive reporter gene constructs in transiently transfected MCF-7 cells. ERE-vit-CAT contains the promoter and flanking regions of the frog vitallogenin-B1 gene upstream of the chloramphenicol-acetyltransferase structural gene. pATC2 contains only the promoter region of the vitallogenin gene and two consensus ERE motifs. pS2-luc contains the regulatory flanking region of the human pS2 gene upstream from the SV40 promoter and the luciferase gene. Our results show that all three reporters were induced by CTr with similar concentration dependency and with 100 nM CTr as effective as 1 nM E_2 (Figure 4, B−D). Co-treatment with CTr did not affect E_2 -induced expression levels. Taken together, these results indicate that the CTr-induced accumulation of mRNA of an endogenous E_2-responsive gene results from increased transcriptional activation and that CTr is equally effective in the activation of simple and complex ERE-containing promoters.

AhR Signaling Pathway. Because of the established effectiveness of orally administered I3C in the induction of CYP450 activities associated with the Ah receptor pathway and the well established role of activation of the Ah receptor in tumor promotion (*31*), we examined the effects of CTr on key indicators of Ah receptor function. We measured the ability of CTr to induce expression of both the CYP1A1-associated EROD activity in MCF-7 cells and of an AhR-responsive DRE-CAT reporter construct containing the promoter and flanking regions of the CYP1A1 gene stably transfected in murine hepatoma Hepa-1c1c7 cells (*15*). As expected (Figure 5), based on the relatively weak binding affinity of CTr for the AhR that we determined previously (*13*), CTr proved in both assays to be a very weak activator as compared to the ICZ positive control treatment.

Taken together, these results indicate that CTr functions as a classical agonist (*32*) of the ER signaling pathway with weak activity toward the AhR signal transduction pathway.

Structural Modeling of CTr Binding to the ER and Comparison with 4-Hydroxytamoxifen. Because CTr is without obvious stuctural similarity to E_2, we conducted a conformational analysis of CTr and computed its theoretical fit into the ER ligand-binding site. A comparison of the expected lowest energy conformation of CTr with conformations of other established ER ligands indicates a remarkable similarity with tamoxifen, a tissue-specific and promoter-specific estrogen antagonist. The structures of CTr and 4-hydroxytamoxifen (OHT) are shown in Figure 6A and Figure 6B, respectively. The portion of each of the molecules that fits into the 3-OH region of the ER ligand-binding site is shown oriented to the left. Of note is that the molecular dimensions of the two molecules are similar. For example, the distance between the C-6 positions of the lower two

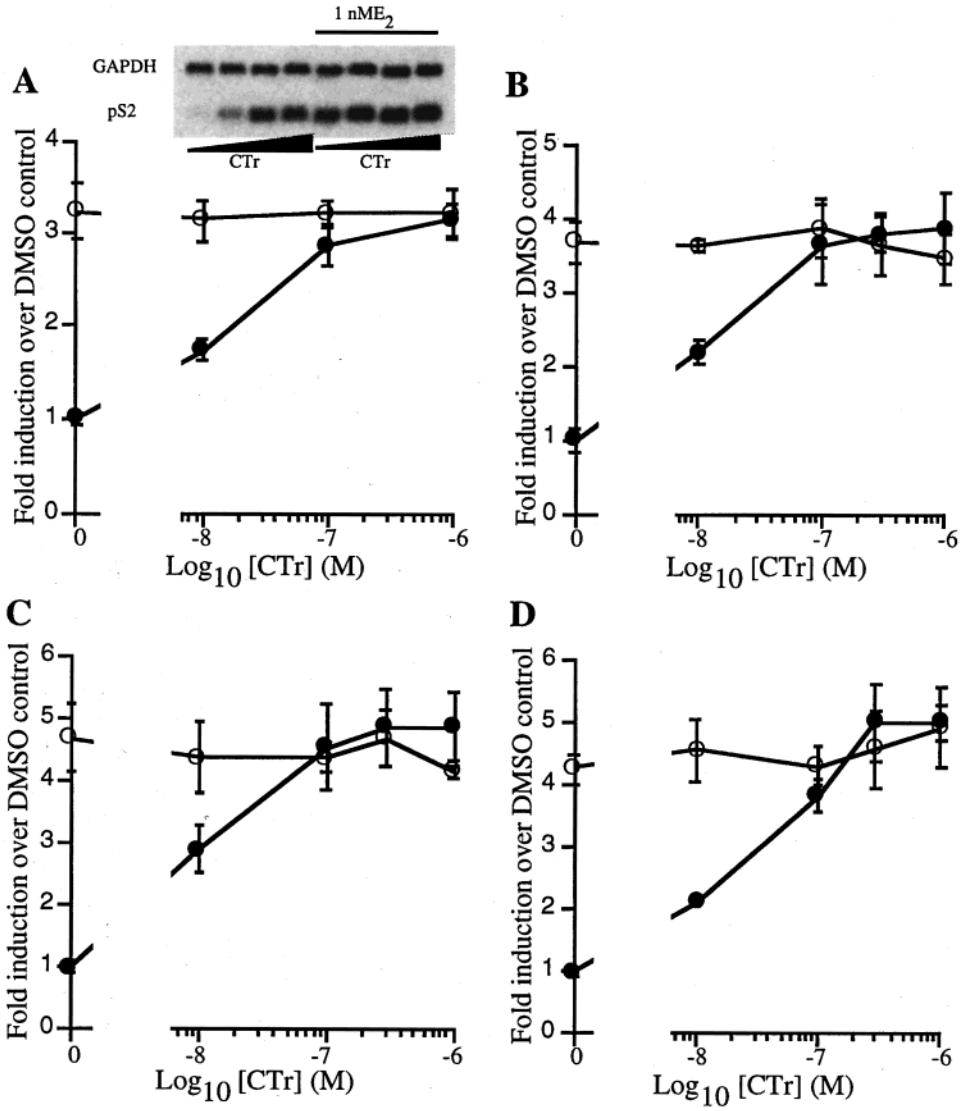

FIGURE 4: Effect of CTr on ER-responsive gene expression. Panel A shows the expression of endogenous pS2; estrogen-depleted MCF-7 cells were treated for 48 h with CTr-1 at concentrations ranging from 0.1 to 10.0 μM, with (open circles) or without (closed circles) E_2 (1 nM). pS2 mRNA levels were measured by Northern-blot analysis and normalized using GADPH mRNA as an internal standard. Results are presented as average and standard deviation of three experiments. A representative Northern blot is shown on top. Panels B, C, and D show transcription activity of reporter genes: MCF-7 cells were transiently transfected with 0.1 μg per plate of pS2-luc (B), or with 1.0 μg per plate of pERE-vit-CAT (C) and pATC2 (D). Transfected MCF-7 cells were treated for 48 h with CTr at concentrations ranging from 0.1 to 10.0 μM, with (open circles) or without (closed circles) E_2 (1 nM). Results are presented as fold induction over the DMSO control, as the average and standard deviation of four independent transfections.

indole moieties indicated in Figure 6A is 20 Å and thedistance of the corresponding hydroxyl carbon and the nitrogen atom in Figure 6B is 22.5 Å; this distance was also found to be 20.4 Å by crystal structure analysis of OHT (*29*). In addition, the aromatic substituents of the two molecules are similarly noncoplanar.

In Figure 6, C and D, we present the same molecules in identical orientations as above, including their solvent-accessible surfaces. The portion of each of the molecules, which fits into the 3-OH region of the ER ligand-binding site is shown oriented to the left. These figures provide a direct geometrical comparison of the properly oriented surfaces as well as a comparison of the polarization-induced charge on their solvent-accessible surfaces. The results indicate a similar charge pattern on the portion of each of the molecules, which fits into the 3-OH region of the binding site. It should be noted that, although only CTr and tamoxifen are shown, all four of the molecules examined, including E_2 and raloxifene, had a similar charge distribution on that region of the surface.

We next investigated the possibility of CTr binding to a site similar to that occupied by OHT in the ER-binding site. In Figure 6 (Panels E and F), we present two views of the overlapping solvent surfaces of the quantum mechanically derived CTr (shown as dots) and the experimentally determined OHT (*29*) (shown as a continuous gray surface), providing a direct comparison of the sizes and shapes of these two molecules. Panel E shows the molecules oriented as in panels A, B, C, and D, and Panel F shows them rotated by 90 degrees along the vertical axis. The OHT pocket is held rigid in these calculations; relaxation of the surrounding molecular environment would allow an even better accommodation of the two structures. The figures provide compelling evidence for the incorporation of CTr into the ER-binding site, both from "steric" (Panels E and F) and electrostatic (Panels C and D) considerations.

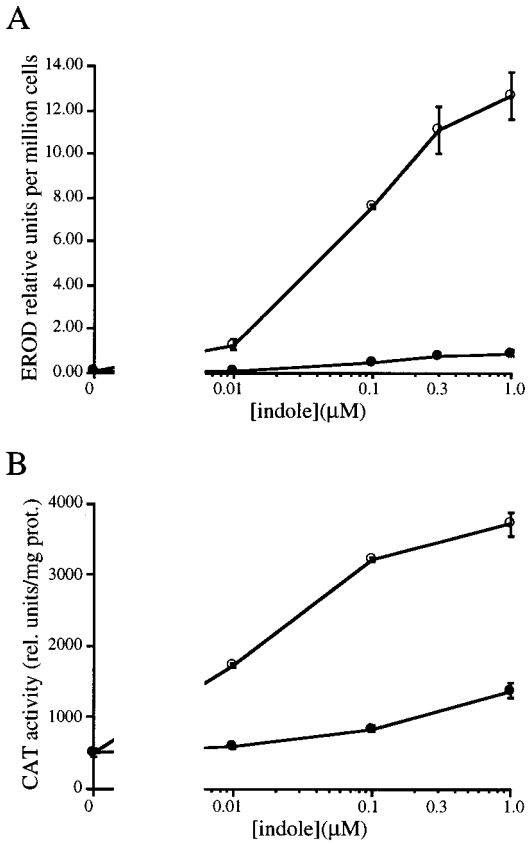

FIGURE 5: Effect of CTr on Ah-Receptor responsive gene expression. (A) Induction of endogenous cytochrome P450-1A1. MCF-7 cells were treated for 24 h with ICZ as a control (open circles) or with CTr (closed circles) at the concentrations indicated and EROD activity was measured. (B) Murine hepatoma cells Hepa-1c1c7 permanently transfected with a DRE-CAT reporter (clone M8) were treated with ICZ (open circles) or CTr (closed circles) at the concentrations indicated for 48 h.

DISCUSSION

Our results show that the novel diet-derived cyclic methylene indole trimer, CTr, behaves as an estrogenic substance in vitro and in cell culture. CTr binds to the ER, activates ER binding to the ERE, and initiates the transcription of an endogenous E_2-responsive gene as well as that of E_2-responsive reporter genes. The activity of CTr in these assays is as high as about 1% that of E_2.

To estimate the physiological significance of CTr production in vivo following oral administration of I3C, an analysis of reported tissue levels of CTr will be helpful. Published work by us and others indicates that the level of CTr produced following oral administration of I3C to rodents is comparable to levels of other major products, DIM and LTr-1. Using Sprague−Dawley rats, we readily detected CTr in the intestinal contents 5 h after treatment (*13*), occurring in about 50% the yield of the other major products. Consistent with these observations, Stresser et al. (*14*) provided chromatographic evidence for the accumulation of I3C acid products including CTr in the liver of Fisher rats 3 h following oral treatment with I3C to levels that again were roughly 50% the levels of DIM and LTr-1. These researchers estimated the levels of each of these major I3C products in rat liver to be in the range of 1−10 μM, which is well in excess of the concentrations (0.1 μM) we find necessary to activate the ER. Thus, it appears that CTr is produced in physiologically significant levels following ingestion of I3C.

Although CTr may attain active concentrations in vivo following administration of I3C, whether CTr contributes to the cancer-protective or cancer-promoting effects of I3C remains to be established. An intriguing possibility is that CTr may contribute to an overall estrogenic effect of oral I3C and that this estrogenic activity may account for the cancer-promoting effects of I3C in liver and for the cancer-protective effects of I3C in mammary glands. Williams et al. reported recently that oral I3C produced estrogenic effects in trout at doses below those required for Ah receptor activation. These investigators suggested that oral I3C may function as do other ER agonists in the promotion of carcinogen-induce liver tumors in the trout and rat models (*11*). CTr might also contribute to the cancer-protective effects of oral I3C against spontaneous mammary tumors by stimulation of mammary gland maturation resulting in decreased susceptibility to carcinogeneis, as suggested recently for the natural cancer-protective agent, genestein (*33*, *34*).

A comparison of the expected lowest energy conformation of CTr with conformations of other established ER ligands indicated a remarkable similarity with tamoxifen, a tissue and promoter specific estrogen antagonist currently under study as a breast cancer therapeutic agent (*35*). We found that the ER ligands compared quantum mechanically all have a similar charge distribution around the boundary region of the molecule that fits into the 3-OH region of the ER-binding site. Furthermore, overlapping surfaces of the CTr with those of experimentally established ligands show very little difference between CTr and tamoxifen, lending provocative evidence in support of the binding of CTr to the ER-binding site.

In light of the marked structural similarity of CTr and tamoxifen with regard to their interactions with the ligand-binding region of the ER, a comparison of the biological activities of CTr with those of tamoxifen and related substances is in order. Published data indicate that OHT, the activated form of tamoxifen, is a potent ligand for the human ER with a binding affinity in the range of 10 nM. In contrast to agonist activity, we observed for CTr, OHT is a potent inhibitor of MCF-7 cell proliferation (IC_{50} = 0.5 nM) (*36*). Whether CTr exhibits tissue and promoter specific agonist activities as does tamoxifen remains to be seen. It is interesting to note, however, that the activities of OHT, and other synthetic ER ligands, are highly dependent on the presence of a hydroxyl group in the position that corresponds to C-4 of tamoxifen (*37*, *38*). Loss of this substituent from OHT results in a 2 orders of magnitude decrease in ER-binding affinity to a level that is similar to the affinity we observe for CTr. This decrease in binding affinity is accompanied by a similar large decrease in potency against MCF-7 cell proliferation to a level of potency that is only about 10-fold greater than the concentration of CTr observed to inhibit MCF-7 cell proliferation (unpublished data). Addition of a hydroxyl group at the appropriate position(s) of CTr may produce a similar pronounced effect on the activity of this natural product. Further studies to explore

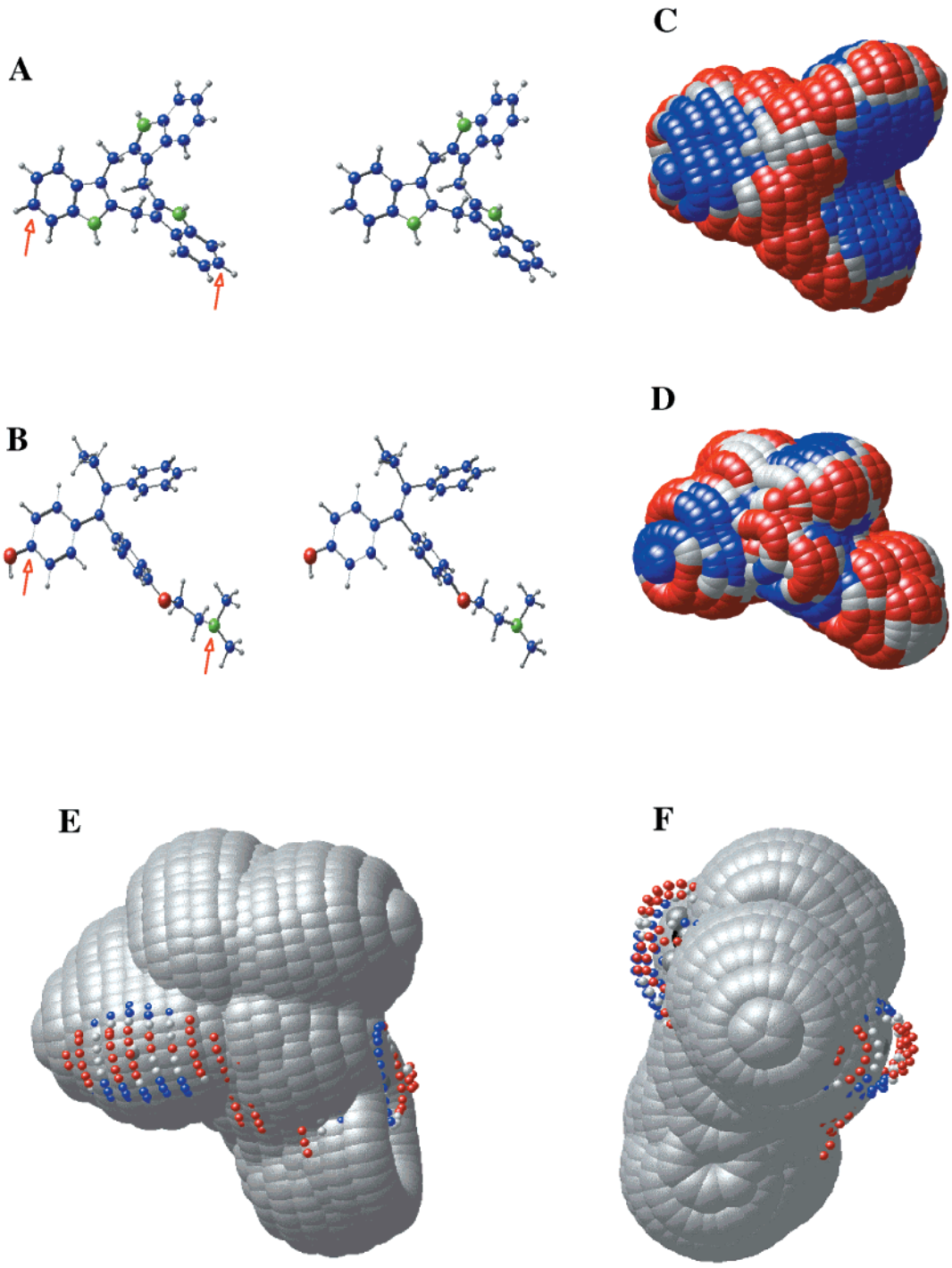

FIGURE 6: Stereoviews of CTr (A) and OHT (B). Structures were determined by quantum mechanical geometry optimization calculations. Comparison of polarization-induced charges on the surfaces of CTr (C) and OHT (D). Construction of a solvent-accessible surface around each of the QM-derived molecules shown in panels A and B allows solution of coupled Schrödinger and Poisson−Boltzmann equations, resulting in the polarization charge on the surface elements due to the aqueous environment. The electronic distribution of the molecule is allowed to rearrange in response to the polarization of its interface, resulting in an accurate depiction of the induced surface charge density. Blue indicates positive surface charge, red indicates negative surface charge, and gray indicates neutral areas. It should be noted that the sign of the surface charge, is essentially opposite that of the charge on the atom below the surface element. Comparison of the sizes and shapes of CTr and OHT. A solvent-accessible surface was created around the crystallographically determined OHT structure, as determined by Shiau et al. (*25*) and is shown as a continuous gray surface; the CTr structure, determined quantum mechanically, is shown as dots. In panel E, the molecules are oriented with the 4-OH of OHT on the left; in panel F, the molecules are rotated by 90 degrees, looking "down" the 4-OH end. The minimum energy conformation of the quantum mechanical CTr in the experimentally determined ER-binding site of OHT was determined by varying position and angular orientation of the CTr molecule within the OHT-binding site, while the atoms comprising the binding site itself were not allowed to relax. Interatomic potentials required for this minimization were determined by pairwise summation using local density methods and reflect the electronic overlap repulsion between the atoms comprising the CTr molecule and those in the receptor-binding site.

the possible metabolic activation and tissue specific activities of CTr and to further define the role of CTr in the cancer modulating activities of I3C are in progress in our laboratories.

REFERENCES

1. Nixon, J. E., Hendricks, J. D., Pawlowski, N. E, Pereira, C. B., Sinnhuber, R. O., and Bailey, G. S. (1984) *Carcinogenesis 5*, 615−619.
2. Tanaka, T., Kojima, T., Morishita, Y., and Mori, H. (1992) *Jpn. J. Cancer Res. 83*, 835−842.
3. Morse, M. A., LaGreca, S. D., Amin, S. G., and Chung, F. L.(1990) *Cancer Res. 50*, 2613−2617.
4. Wattenberg, L. W., and Loub, W. D. (1978) *Cancer Res. 38*, 1410−1415.
5. Grubbs, C. J., Steele, V. E., Casebolt, T., Juliana, M. M., Eto, I., Whitaker, L. M., Dragnev, K. H., Kellof, G. J., and Lubet, R. L. (1995) *Anticancer Research 15*, 709−716.
6. Bradlow, H. L., Michnovicz, J. J., Telang, N. T., and Osborne, M. P. (1991) *Carcinogenesis 12*, 1571−1574.
7. Kojima, T., Tanaka, T., and Mori, H. (1994) *Cancer Res. 54*, 446−1449.
8. Pence, B., Buddingh, H., and Yang, S. (1986) *J. Natl. Cancer Inst. 77*, 269−276.
9. Bailey, G. S., Hendricks, J. D., Shelton, K. W., Nixon, J. E., and Pawlowski, N. E. (1987) *J. Natl. Cancer Inst. 78*, 931−936.
10. Kim, D., Han, B., Ahn, B., Hasegawa, R., Shirai, T., Ito, N., and Tsuda, H. (1997) *Carcinogenesis 18*, 377−381.
11. Oganesian, A., Hendricks, J., Pereira, C., Orner, G., Bailey, G., and Williams, D., (1999) *Carcinogenesis 20*, 453−458.
12. Grose, K. R., and Bjeldanes, L. F. (1992) *Chem. Res. Toxicol. 5*, 188−193.
13. Bjeldanes, L. F., Kim, J. Y., Grose, K. R., Bartholomew, J. C. and Bradfield, C. A. (1991) *Proc. Natl. Acad. Sci. U.S.A. 88*, 9543−9547.
14. Stresser, D. M., Williams, D. E., Griffin, D. A., and Bailey, G. S. (1995) *Drug Metab. Disposition 23*, 965−975.
15. Chen, Y.-H., Riby, J., Srivastava, P., Bartholomew, J., Denison, M., and Bjeldanes, L. (1995) *J. Biol. Chem. 270*, 22548−22555.
16. Chen, I., Safe, S., and Bjeldanes, L. (1996) *Biochem. Pharm. 51*, 1069−1076.
17. Stresser, D. M., Bjeldanes, L. F., Bailey, G. S., and Williams, D. E. (1995) *J. Biochem. Toxicology 10*, 191−201.
18. Chen, I., McDougal, A., Wang, F., and Safe, S. (1998) *Carcinogenesis 19*, 1631−1639.
19. Chang, Y.-C., Riby, J., Chang, G., Peng, B., Firestone, G., and Bjeldanes, L. (1999) *Biochem. Pharm. 58*, 825−834.
20. Santell, R. C., Chang, Y. C., Nair, M. G., and Helferich, W. G. (1997) *J. Nutr. 127*, 263- 269.
21. Chang, T., Nardulli, A. M., Lew, D., and Shapiro, D. J. (1992) *Mol. Endocrinol. 6*, 346- 354.
22. Gillesby, B. E., Stanostefano M., Porter, W., Safe, S., Wu, Z. F., and Zacharewski, T. R. (1997) *Biochemistry 36*, 6080−6898.
23. Reese, J. C., and Katzenellenbogen, B. S. (1991) *Nucl Acids Res 19*, 6595−6602.
24. Seed, B., and Sheen, J. Y. (1988) *Gene 67*, 271−277.
25. Schmidt, M. W., Baldridge, K. K., Boatz, J. A., Elbert, S. T., Gordon, J. S., Jensen, J. J., Koseki, S., Matsunaga, N., Nguyen, K. A., Su, S., Windus, T. L., Dupuis, M., and Montgomery, J. A. (1993) *J. Comput. Chem. 14*, 1347−1363.
26. Wilson, W. D., Schaldach, C. M., and Bourcier, W. L. (1997) *Chem. Phys. Lett. 267*, 431−437.
27. Frisch, M. J., Head-Gordon, M., and Pople, J. A. (1990) *Chem. Phys. Lett. 166*, 275−280).
28. Brzozowski, A. M., Pike, A., Dauter, Z., Hubbard, R. E., Bonn, T., Engstrom, O., Ohman, L., Greene, G. L., Gustafsson, J.-A., and Carlquist, M. (1997) *Nature 389*, 753−758.
29. Shiau, A. K., Barstad, D. Loria, P. M., Cheng, L, Kushner, P. J., Agard, D. A., and Greene, G. L. (1998) *Cell 95*, 927−937.
30. Wilson, W. D., and Schaldach, C. M. (1998) *J. Colloid Interface Sci. 208*, 546−554.
31. Schmidt, J. V., and Bradfield, C. A. (1996) *Annu. Rev. Cell Dev. Biol. 12*, 55−89.
32. Wehling M. (1995) *J. Mol. Med. 73*, 439−47.
33. Hsieh, C. Y., Santell, R. C., Haslam, S. Z., and Helferich, W. G. (1998) *Cancer Res. 58*, 3833−3838.
34. Lamartiniere, C. A., Moore, J. B., Brown, N. M., Thompson, R., Hardin, M. J., and Barnes, S. (1995) *Carcinogenesis 16*, 2833−2840.
35. Watanabe, T., Inoue, S., Ogawa, S., Ishii, Y., Hiroi, H., Ikeda, K., Orimo, A., and Muramatsu, M. (1997) *Biochem. Biophys. Res. Comm. 236*, 140−145.
36. Grese, T., Sluka, J., Bryant, H., Cullinan, G., Glasebrook, A., Jones, C., Matsumoto, K., Palkowitz, A., Sato, M., Termine, J., Winter, M., Yang, N., and Dodge, J. (1997) *Proc. Natl. Acad. Sci. U.S.A. 94*, 14105−14110.
37. Grese, T. A., Cho, S., Finley, D. R., Godfrey, A. G., Jones, C. D., Lugar III, C. W., Martin, M. J., Matsumoto, K., Pennington, L., Winter, M., Adrian, M., Cole, H., Magee, D., Phillips, D., Rowley, E., Short, L., Glasebrook, A., and Bryant, H. (1997) *J. Med. Chem. 40*, 146−167.
38. Biberger, C., and von Angerer, E. (1996) *J. Steroid Biochem. Mol. Biol. 58*, 31−43

BI9919706